

Introducing Energy Efficient Routing in UAV-Satellite NTN for Dynamic 6G Interconnectivity

George Amponis, *Graduate Student Member, IEEE*, Thomas Lagkas, *Senior Member, IEEE*, Pavlos Bouzinis, Panagiotis Radoglou-Grammatikis, *Member, IEEE*, Antonios Sarigiannidis, Panagiotis Sarigiannidis, *Member, IEEE*, and Vasileios Argyriou

Abstract—The integration of Unmanned Aerial Vehicles (UAVs) and Low-Earth Orbit (LEO) satellites as aerial nodes in non-terrestrial networks (NTNs) presents both opportunities and challenges for on-demand 6G interconnectivity. This paper presents a new Composite Cost Metric (CCM) which improves energy-efficient routing performance in combined UAV-satellite constellations. We consider incorporating cumulative Free Space Path Loss (FSPL) and residual energy into the route selection process for both proactive and reactive protocols, our approach refines the routing decisions of classical protocols. The proposed CCM-driven modifications and protocol-specific integration typologies can improve overall route stability, reduce energy consumption per delivered packet, and optimize network reliability by dynamically selecting relays with lower attenuation and higher energy availability. We develop an NS-3-based simulation framework that integrates realistic satellite orbital mechanics, UAV mobility models, and a hybrid energy model that includes solar energy harvesting for satellites. Simulation results demonstrate that our enhancements can indeed outperform baseline implementations in packet delivery ratio, energy efficiency, and end-to-end delay which makes them viable for next-generation NTN-supported 6G networks, at the expense of some additional control overhead. With this set of developments we aim to pave the way for global-optimum and energy-aware emergency and disaster relief communications.

Index Terms—LEO Constellations, Multi-Altitude Flying Ad-hoc Networks (FANETs), Aerial Base Stations, Satellite-Drone Relaying, Energy-Aware Routing, Non-Terrestrial Networks, 6G Connectivity.

This project has received funding from the European Union's Horizon Europe research and innovation programme under grant agreement No. 101097122 (ACROSS). Disclaimer: Funded by the European Union. Views and opinions expressed are however those of the author(s) only and do not necessarily reflect those of the European Union or European Commission. Neither the European Union nor the European Commission can be held responsible for them.

Corresponding author: Pavlos Bouzinis

George Amponis is with the Dept. of R&D, K3Y Ltd., Sofia, Bulgaria, and the Dept. of Informatics, Democritus University of Thrace, Kavala Campus, Greece (email: gamponis@k3y.bg, gamponis@cs.duth.gr). Thomas Lagkas is with the Dept. of Informatics, Democritus University of Thrace, Kavala Campus, Greece (e-mail: tlagkas@cs.duth.gr). Pavlos Bouzinis is with MetaMind Innovations P.C., 50100 Kozani, Greece, Thessaloniki, Greece (e-mail: pbouzinis@metamind.gr). Panagiotis Radoglou-Grammatikis is with the Dept. of R&D, K3Y Ltd., Sofia, Bulgaria, and the Dept. of Electrical and Computer Engineering, University of Western Macedonia, Kozani, Greece (e-mail: pradoglou@k3y.bg, pradoglou@uowm.gr). Antonios Sarigiannidis is with the Dept. of R&D, K3Y Ltd., Sofia, Bulgaria (e-mail: asarigia@k3y.bg). Panagiotis Sarigiannidis is with the Dept. of Electrical and Computer Engineering, University of Western Macedonia, Kozani, Greece (e-mail: psarigiannidis@uowm.gr). Vasileios Argyriou is with the Dept. of Networks and Digital Media, Kingston University, London, UK (e-mail: vasileios.argyriou@kingston.ac.uk).

I. INTRODUCTION

THE integration of Unmanned Aerial Vehicles (UAVs) into Low-Earth Orbit (LEO) satellite networks represents a critical threshold for next-generation wireless solutions. Strategic relay selection in these hybrid 6G environments creates a paradigm that enhances communication range on-demand while maximizing network capabilities. Our work studies how optimizing relay selection enhances performance—predominantly from an energy perspective—alongside overall communication network robustness in UAV-LEO Multi-Altitude Constellations. We delve into the potential trade-offs, networking implications, and solutions to relay selection optimization problems that the industrial and research landscape will face as on-demand and mission-critical communications become prevalent.

UAVs operating as network nodes have transformed traditional mobile base stations into dynamic elements for communication networks. LEO satellites represented by Starlink with its specific orbital parameters demonstrate a solid answer to the increasing need for widespread high-speed connectivity inside 6G networks. High-altitude platforms (HAPs) together with FANETs form a complicated yet optimally efficient system for future communication requirements when integrated with satellite constellations. The successful implementation of this system depends on optimized relay selection that accounts for UAV battery performance together with signal propagation delay and the changing dynamics of aerial and spaceborne nodes. Mobile Ad-hoc Networks (MANETs) have brought significant changes to decentralized and dynamic deployments by revolutionizing their communication capabilities. The introduction of hybrid UAV and LEO satellite networks into advanced technological frameworks requires upgrading traditional MANET routing protocols, which tend to encounter significant challenges.

a) Dynamic Topology, High Mobility, and Energy Constraints: Hybrid NTNs exhibit extreme node mobility and continuously shifting topologies, making routing a complex and energy-intensive task. Traditional MANET protocols struggle to maintain consistent route information due to frequent topology changes, leading to excessive control overhead, route instability, and increased energy consumption. In UAV-LEO constellations, the high velocity of satellites and intermittent connectivity introduce additional challenges, exacerbating link

disruptions and requiring frequent route recalculations. Conventional routing strategies fail to account for the compounded impact of mobility and energy constraints, where UAVs must optimize transmission power and relay selection to sustain network longevity. Addressing these issues necessitates routing mechanisms that integrate predictive topological adaptation with energy-aware link selection, ensuring stability while minimizing energy expenditure across dynamic, multi-altitude architectures.

b) Heterogeneous Link Characteristics and Energy-Optimized Routing: UAV-LEO networks operate over highly heterogeneous links, combining UAV-based ad hoc relaying with satellite-based long-range connectivity. These network segments exhibit distinct physical and energy-related constraints: UAVs are energy-constrained and require power-efficient routing strategies, while LEO satellites introduce high-latency, dynamically shifting link characteristics influenced by orbital mechanics. Conventional routing protocols fail to integrate these disparate constraints, leading to sub-optimal path selection that disregards both energy sustainability and link stability. Effective routing solutions for UAV-LEO networks must incorporate composite cost metrics that jointly consider free-space path loss, energy availability, and link reliability, ensuring that relay selection maximizes transmission efficiency while extending the operational lifespan of energy-limited nodes. Energy efficiency is critical, particularly for UAVs implementing communication relaying in critical environments [1]. The majority of relevant routing protocols fail to prioritize energy optimization when making decisions which results in sub-optimal path selection energy-wise. Energy-aware routing decisions represent an essential requirement because they determine how long UAVs survive in the network and how effective they remain throughout their operation. The vast separation between satellites and ground nodes creates long delays and unpredictable bandwidth conditions and special topology limitations. Traditional protocols are not designed to handle discrepancies stemming from the "marriage" of aerial ad hoc networks with space-born counterparts, with a distance spanning hundreds of thousands of meters, which often leads to inefficient routing decisions and poor utilization of the available resources [2]. Critical applications enabled by UAV-LEO network hybrids need smart protocols to achieve a "global optimum". Increased mobility, scale, and link parameter heterogeneity demand advanced solutions capable of adapting to changing network conditions while ensuring efficient, secure, and reliable communication. This sets the stage for the development of innovative routing protocols that leverage the CCM to intelligently determine the optimal path, effectively balancing the trade-offs between immediacy, reliability, and resource consumption. Control-message enhancements specific to UAV-LEO satellite communications were also considered by D. Shumeye Lakew et al. [3] as a means of bringing about seamless coverage in 6G.

For comparative baselines, we include Ad-hoc On-demand Multipath Distance Vector (AOMDV) [4], [5] and a Cyber-Physical Routing protocol exploiting Trajectory Dynamics (CPR-TD) [6]. The main contributions of this paper consist of three parts which focus on improving energy-efficient routing

mechanisms for UAV-assisted cellular networks that integrate LEO satellites. First, we introduce enhanced versions of the OLSR and AODV protocols, integrating our CCM to enable multi-criteria route selection based on residual energy and estimated link quality; these modifications do indeed go beyond traditional routing protocol implementations, embedding energy-awareness and link attenuation directly into routing decisions (calculated discreetly in each case) with the purpose of addressing the nature and challenges of heterogeneous NTN. Second, we propose a comprehensive simulation framework built on the NS-3 platform, incorporating real-world satellite orbital dynamics (particularly regarding the Starlink constellation), UAV mobility patterns, and a new energy model, providing a robust testbed for evaluating the performance of energy-efficient routing protocols in diverse scenarios. Third, as hinted above, we extend the native NS-3 core energy source and model classes (discussed in detail in Subsection V), and introduce a composite model which integrates the standard energy source with a solar energy harvesting mechanism which is applicable to LEO-satellite constellations for greater realism. The described contributions form a platform to evaluate routing in NTN scenarios. We begin by developing our proposal from OLSR and AODV before implementing our new metric for enhancement. The modifications made to OLSR and AODV protocols use their fundamental structures to incorporate the CCM in different ways. The CCM metric in OLSR gets implemented through the willingness parameter which leads to MPR selection modifications based on link and energy parameters and replaces the ETX metric which we consider as a baseline). Similarly, AODV uses CCM as a replacement for ETX in RREQ and RREP messages to enable nodes to select routes based on their cumulative FSPL and residual energy during route discovery operations. Our performance evaluation uses AODV-ETX and OLSR-ETX as primary baselines, and includes AOMDV and CPR-TD as additional state-of-the-art comparators, to demonstrate CCM metric advantages across diverse routing paradigms. The selection of AODV-ETX over vanilla AODV is deliberate because ETX provides an effective link reliability assessment through expected transmission count estimation which better suits dynamic UAV-satellite environments. Likewise, OLSR-ETX offers a fairer baseline than hop-count-only OLSR when assessing link-aware energy efficiency.

II. RELATED WORK

D. Huo, Q. Liu, Y. Sun, and H. Li in [7] focus on optimizing network performance in large-scale satellite swarm systems. The paper addresses challenges like fast node movement, long communication distances, and dynamic topologies. The paper proposes an inter-satellite routing protocol, IS-OLSR, based on the traditional MANET protocol OLSR. This protocol aims to improve network performance by implementing subnet division, abstraction, and gateway election. IS-OLSR has been shown through simulations to significantly reduce routing overhead as well as data transmission delay. The study is relevant in the context of satellite network communication technologies, especially in fields such as cross-region communication, disaster relief, and national defense.

H. Liming et al in [8] propose a novel load-balancing strategy for routing in LEO satellite constellations. Their approach focuses on optimizing the traffic distribution across the network by considering historical traffic data of satellite links. This method significantly improves network congestion and packet loss issues in high-traffic areas, enhancing overall network performance. The paper emphasizes the relevance of managing traffic effectively in the dynamic topology of LEO satellite networks, particularly for space-based IoT networks. The authors employ simulation studies to demonstrate the efficacy of their proposed load-balancing method in reducing delay performance degradation and packet loss under high-load conditions. Z. Liu et al. in [9] composed a research which focuses on addressing the challenges of uneven satellite network load and unstable link connections. The authors propose a globally adaptive satellite network routing strategy, G-AODV, which enhances the existing Ad hoc On-Demand Distance Vector Routing (AODV) protocol by incorporating a traffic prediction mechanism during the route discovery phase. This strategy aims to avoid heavily loaded nodes from becoming intermediate nodes and introduces a path replacement strategy to replace paths before node congestion occurs, achieving load balancing. The paper also discusses the highly volatile (and occasionally completely unpredictable) nature of satellite link instability and its impact on maintaining a consistent communication environment. The study is significant in improving satellite network routing efficiency, particularly in dynamic and complex network environments. S. Suhaimi, K. Mamat, and K. Daniel Wong in [10] propose a method to improve the Optimized Link State Routing (OLSR) protocol in mobile ad-hoc networks (MANETs) by considering battery power status. The study emphasizes the relationship between power status and OLSR's functionality, particularly in maximizing the use of battery power sources. It involves modifications to the OLSR source code to enhance node 'willingness' based on battery power status, demonstrating the improved utilization of battery resources in MANETs through experiments. The paper also discusses the significance of energy awareness in wireless ad hoc networks and proposes methods for optimizing power usage in OLSR, especially when nodes rely on battery power in infrastructure-free scenarios. S. Jiao et. al. in [11] focus on the deployment of LEO satellite networks with inter-satellite links. These networks have gained significant attention due to their high throughput, wide coverage, and cost-effective control and management. This paper particularly emphasizes the role of these networks in supporting 5G mobile services (and potentially 6G in the future), acting as a space bearer to connect distant users with the ground core network. The authors propose an architecture for the space bearer network and develop routing protocols and signaling methods to address challenges like large-scale flooding and prolonged routing convergence. Moreover, they introduce coordinated signaling techniques across different network segments to ensure Quality of Service (QoS) consistency. The experimental validation of their routing design demonstrates successful User Equipment (UE) to UE connections, highlighting the paper's contribution to advancing satellite-based 5G networks.

To position our study within broader NTN and Space-

Air-Ground Integrated Network (SAGIN) developments, we reference recent works on real-time large-scale satellite-UAV systems [12], maritime hybrid Satellite-UAV-terrestrial architectures [13], and cell-free Satellite-UAV networks for wide-area IoT [14]. From a UAV communications viewpoint, the UAV-to-Everything (U2X) paradigm [15] generalizes beyond D2D and motivates our protocol-agnostic CCM integration across proactive and reactive stacks. Finally, energy-aware satellite-terrestrial computing [16] and LEO-focused SAGIN outlooks [17] further underline the importance of jointly optimizing link quality and energy sustainability in heterogeneous non-terrestrial networks.

Recent advancements in NTN and Flying Ad-Hoc Networks (FANETs) have further highlighted the need for sophisticated routing strategies. Dong et al. [18], [19] provide stochastic-geometry models for analyzing uplink performance in heterogeneous non-terrestrial networks, offering critical insights under harsh conditions. For highly dynamic FANETs, Yang et al. [20] proposed a betweenness centrality-based DSR variant, while Wang et al. [21] introduced a hybrid proactive-reactive ant-colony routing protocol with link quality prediction. Furthermore, Hu et al. [6] developed a cyber-physical routing protocol that leverages trajectory dynamics for mission-oriented FANETs. These studies underscore the trend toward more intelligent, context-aware routing, yet they often focus on either the satellite or the aerial layer in isolation. Our CCM complements this body of work by providing a protocol-agnostic, pluggable metric that captures a global energy-attenuation optimum across heterogeneous links.

A significant research gap persists in the integration of these advancements with the dynamic and energy-intensive characteristics of hybrid networks between UAV deployments and LEO satellite constellations. Current methodologies often overlook the compounded complexity brought by the integration of aerial and satellite components, especially in terms of energy efficiency and the adaptability of routing protocols in high-mobility environments. This work, introducing CCM integrated into routing protocols with different core route selection algorithms (namely AODV and OLSR in this study), addresses this gap because it uniquely combines and couples considerations for energy efficiency, link stability, and the distinct attributes of satellite and UAV communications in scenarios of communication range extension.

III. BACKGROUND

This section is dedicated to the analysis of two considered ad hoc routing protocols, both of which have constituted the basis of a significant amount of developments targeting similar environments. Moreover, this section targets the analysis of matters relevant to LEO satellite constellations' orbital mechanics and the modelling of FSPL for such wireless links. Figure 1 visualizes the envisioned communications relaying paradigm leveraging dynamic satellite backhauls. The choice of AODV-ETX and OLSR is deliberate: AODV-ETX, an advanced version of AODV, focuses on link quality, similar to CCM's goals while the default implementation of OLSR offers a proactive routing perspective, contrasting AODV's reactive

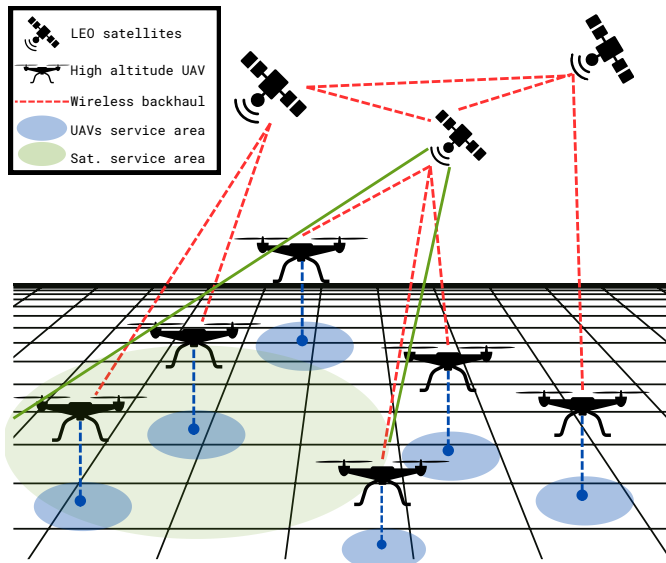


Figure 1: Envisioned use-case of hybrid UAV-LEO satellite-enabled relaying

nature. Header overheads comparability was also a factor we considered, in order to ensure a fair assessment of CCM's impact on network performance.

In the context of both OLSR and AODV (and their subsequent enhancements), we refer to networked entities as "nodes". This includes UEs, UAVs, and LEO satellite relays. The modeled system represents a hybrid network topology comprising the above-mentioned entities, interconnected through a single routing protocol across all link types. UEs are ground-based devices that communicate with UAVs, which act as aerial relays, while LEO satellites provide backhaul connectivity and facilitate inter-node communication across broader distances. The network operates with a hierarchical structure where UAVs connect UEs to satellites or other UAVs, depending on the route selected. Path selection is influenced by the composite cost metric.

a) *Expected Transmission Count (ETX)*: Traditional routing protocols often use hop count as the primary metric for route selection. However, hop count doesn't account for the link quality. ETX provides a more nuanced metric that considers the loss rate of links, which can lead to the selection of more reliable and higher-throughput routes. ETX considers the transmission success rate, factoring in aspects like packet loss, which is vital when dealing with varying signal qualities in UAV networks. Implementing ETX in AODV for UAVs would ensure that routes are not just the shortest but the most reliable, leading to enhanced data transmission quality. We use ETX [22] as the link-quality baseline. For a link (u, v) with forward and reverse delivery ratios (d_f, d_r) , the per-link ETX is

$$\text{ETX}(u, v) = \frac{1}{d_f \cdot d_r}, \quad d_f, d_r \in (0, 1]. \quad (1)$$

For a path p , the cumulative cost is the sum of link ETX values. Integration follows protocol semantics: in OLSR-ETX, Dijkstra runs on ETX-weighted links; in AODV-ETX, RREQs

accumulate per-link ETX and the RREP returns the minimum-ETX route.

A. The OLSR Protocol

OLSR is a proactive routing protocol for mobile ad hoc networks, standardized in RFC 3626 [23]. Unlike AODV (analyzed in the next subsection), which seeks routes on demand, OLSR continuously maintains routes to all destinations in the network. It achieves efficiency through the use of Multipoint Relays (MPRs) to minimize flooding of control traffic. MPRs are selected nodes that forward broadcast messages during the flooding process. This reduces the number of transmissions required and optimizes the control traffic overhead. Equation (3) formally describes the MPR selection process for two-hop neighbors. For multi-hop routing, this principle is extended by recursively selecting MPRs to cover all nodes in the network, forming a tree that minimizes control traffic overhead while maintaining full routing information, as detailed in the standard. Equation (3) formally describes the MPR selection process using set theory, where $\text{MPR}(s)$ is the set of Multipoint Relays selected by node s . Firstly, let $\mathcal{N}(s)$ denote the one-hop neighbors of a node s . Following that, $\mathcal{N}_2(s)$ denotes the two-hop neighbors of s , which are the neighbors of s 's neighbors but not directly connected to s . More formally, $\mathcal{N}_2(s)$ can be defined as

$$\mathcal{N}_2(s) = \left(\bigcup_{m \in \mathcal{N}(s)} \mathcal{N}(m) \right) \setminus \mathcal{N}(s), \quad (2)$$

indicating that $\mathcal{N}_2(s)$ consists of the neighboring nodes of s 's neighbors, i.e., $\mathcal{N}(m), m \in \mathcal{N}(s)$, while excluding nodes that can be reached from s , i.e., $\mathcal{N}(s)$. The optimal $\text{MPR}^*(s)$ set is described as the smallest possible subset $\mathcal{M} \subseteq \mathcal{N}(s)$, such that all two-hop neighbors of s can be reached through the subset of one-hop neighbors \mathcal{M} . This gives rise to the following minimization problem

$$\text{MPR}^*(s) = \underset{\mathcal{M} \subseteq \mathcal{N}(s)}{\text{argmin}} \left\{ |\mathcal{M}|, \quad \text{s.t.}, \quad \bigcup_{m \in \mathcal{M}} \mathcal{N}(m) \supseteq \mathcal{N}_2(s) \right\}, \quad (3)$$

where $|\mathcal{M}|$ denotes the cardinality of \mathcal{M} .

a) *Efficiency in Dynamic Networks*: The dynamic nature of UAV-enabled networks, characterized by frequent topological changes, demands an adaptive and efficient routing protocol. OLSR, with its proactive routing strategy, is well-suited for such environments. However, the key to its efficiency lies in the strategic selection of Multipoint Relays (MPRs). In UAV-assisted networks, MPRs are dynamically chosen based on current network conditions and node mobility. This approach ensures that the control traffic is minimized, and the routes are quickly established and maintained despite potential changes in nodes' locations.

b) *Control Messages in OLSR*: OLSR disseminates local and global topology using periodic control messages:

- 1) HELLO: Link sensing and neighbor discovery/status.
- 2) TC (Topology Control): Advertises MPR selectors to build the topology graph.
- 3) MID: Declares multiple interfaces when present.

c) *Route Computation Model*: The route calculation in OLSR can be mathematically modeled as finding the shortest path in a graph. In the hop-count formulation, this is described as

$$\text{Route}(s, d) = \min_{p \in \mathcal{P}_{s,d}} \{\text{Length}(p)\}, \quad (4)$$

where $\text{Route}(s, d)$ is the shortest path from s to d , $\mathcal{P}_{s,d}$ denotes the set of all possible paths from s to d , and $\text{Length}(p)$ is the length of the path p , calculated using hop count.

d) *Scalability and Control Overhead*: As networks grow in scale, managing control traffic becomes crucial to maintain network performance. OLSR's MPR system inherently reduces the number of transmissions required for route discovery and maintenance. However, in large-scale UAV networks, even this optimized approach can lead to significant overhead. Techniques such as adaptive control message intervals, MPR selection based on node density, and region-based MPR clustering can be explored to enhance scalability and reduce control traffic further.

B. The AODV Routing Protocol

The AODV routing protocol, standardized in RFC 3561 [24], is designed for mobile ad hoc networks and provides an efficient routing mechanism that establishes routes between nodes only as desired by source nodes. It belongs to the family of Distance Vector routing protocols and uses a sequence number to ensure the freshness of routes and prevent routing loops. On a message-exchange level, the protocol works as follows.

a) *Efficiency in Dynamic Networks*: AODV exhibits particular efficiency in dynamic networks, a characteristic paramount in the volatile topology of UAV-assisted 6G environments and LEO satellite networks. AODV's on-demand nature allows it to adapt swiftly to frequent changes, as routes are established only when required, significantly reducing the overhead associated with maintaining a full map of the network at all times. By minimizing the route discovery frequency through the utilization of sequence numbers and maintaining up-to-date routes to active destinations, AODV can effectively manage the balance between the need for up-to-date path information and the desire to minimize signaling traffic. Furthermore, its ability to quickly respond to link breaks with Route Error (RERR) messages and efficiently establish new routes through Route Requests (RREQs) and Route Replies (RREPs) makes it well-suited for environments where network topology is subject to frequent and unpredictable changes. As such, AODV stands out as a robust solution for ensuring communication reliability and maintaining consistent performance in highly dynamic and mobile network settings.

b) *Control Messages in AODV*: AODV operation centers on three control messages:

- 1) RREQ: Route discovery broadcast from the source when no valid route is known. Includes source/destination addresses, broadcast ID, and sequence numbers.
- 2) RREP: Unicast reply from destination or an intermediate node with a fresh enough route; carries destination sequence number and hop count.

- 3) RERR: Error notification when a link break invalidates active routes, triggering local repair or new discovery.

c) *Route Computation Model*: As seen in Equation (5), the path discovery process is a simple optimization problem, where AODV selects the path with the minimum cost.

$$\text{Route}(S, D) = \min_{p \in \mathcal{P}_{SD}} \{\text{Cost}(p)\} \quad (5)$$

where:

- Route(S, D) = Optimal path from S to D
- \mathcal{P}_{SD} = The set of all possible paths from S to D
- Cost(p) = Cost of p , calculated based on hop count.

AODV maintains routes as long as they are active. If a link break is detected, a RERR message is used to notify affected nodes.

In LEO satellite constellations and similar high-mobility environments:

- 1) *Adaptiveness*: ETX adapts to changing link conditions in real-time, providing a more reliable and consistent network experience.
- 2) *Throughput Optimization*: By avoiding low-quality links, ETX can improve end-to-end throughput, which is crucial for bandwidth-sensitive applications.
- 3) *Approximation of cross-layering*: The ETX metric builds upon statistical metrics inherent to the routing layer and presents a statistically significant tool to compute the expected number of (re)transmissions at the Medium Access Control (MAC) layer.

d) *Scalability and Control Overhead*: AODV scales well in dynamic settings by avoiding global state, but frequent discoveries and repairs increase signaling under high mobility. Using ETX as the baseline path metric reduces retransmissions and helps contain overhead; CCM integration further stabilizes routes at the cost of larger control payloads. Parameter tuning (e.g., ring search TTL, local repair) is important to balance responsiveness and overhead.

C. Orbital Mechanics Overview

For completeness, we briefly outline the orbital-mechanics concepts that underpin the LEO satellite positions used in our simulations. Each satellite follows a nearly circular low-Earth orbit (Starlink-like, altitude $h = 550$ km). The instantaneous radius is therefore $r \approx R_E + h$ where $R_E = 6378$ km is Earth's radius. The orbital period follows from Kepler's third law,

$$T = 2\pi \sqrt{\frac{(R_E + h)^3}{GM}},$$

with $GM = 3.986 \times 10^{14} \text{ m}^3 \text{ s}^{-2}$, yielding $T \approx 95$ min. Satellite positions at simulation time t are obtained from the true anomaly $\nu(t) = 2\pi t/T$ and standard ECI rotations (see Figure 2).

The large slant range between a UAV at altitude 300 m and a LEO satellite motivates the use of the Friis free-space path-loss model which, for carrier frequency $f = 1.8$ GHz and range d , is

$$\text{FSPL}_{\text{dB}} = 20 \log_{10}(d) + 32.44 + 20 \log_{10}(f_{\text{GHz}}). \quad (6)$$

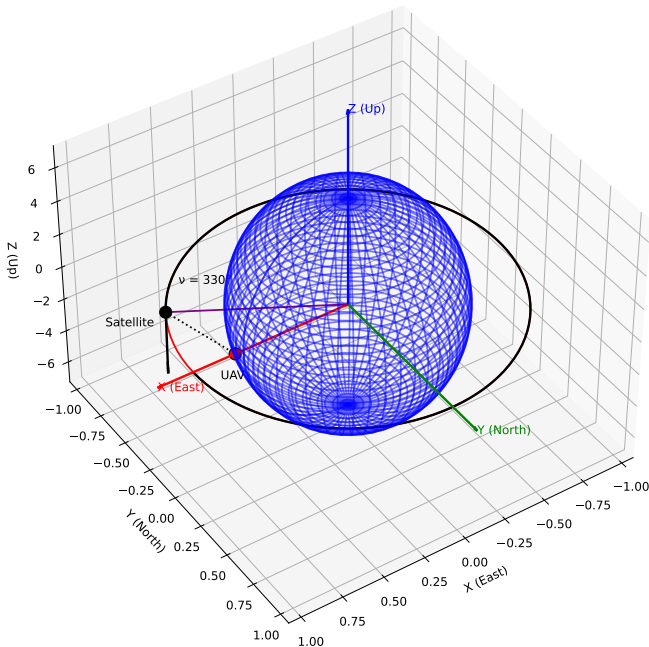


Figure 2: Visualization of LEO satellite on a circular orbit with a 330 deg true anomaly (not true to scale)

These FSPL values feed directly into the cost metric (Eq. 7) and thus influence route selection without requiring more intricate propagation models. Sensitivity to shadowing and fading is captured separately by the physical-layer error model in NS-3 as discussed in Section V.

IV. PROPOSED METHOD

This section outlines a proposed routing protocol designed to tackle the intrinsic challenges posed by such a complex system. Central to this approach is the implementation of the CCM, which dynamically calculates and selects the optimal path for data transmission. Unlike traditional methods, this advanced protocol doesn't just consider a single metric but rather a combination of several crucial factors, each representing a different dimension of the communication link. The CCM incorporates elements such as energy efficiency, link stability, and the specific characteristics of satellite and UAV links. By considering end-to-end delay, the protocol ensures that time-sensitive information is prioritized, addressing the critical latency issues that often plague satellite communications. Energy efficiency is another vital component, particularly for UAVs where battery life is a premium. Optimizing routes based on energy consumption can significantly prolong operational time and enhance the overall sustainability of the network. Link stability is a dynamic factor, especially in a network characterized by high mobility and variable environmental conditions. The CCM takes into account the stability of each link, preferring routes that offer consistent performance over those that might lead to frequent disconnections or require constant rerouting. This aspect is particularly crucial in maintaining a reliable communication standard, essential for applications requiring a consistent data stream. In scenarios where direct UAV-to-UAV communication is feasible and

efficient, the system might minimize the use of satellite links, reducing latency and preserving bandwidth for scenarios where such links are indispensable. Conversely, when satellite paths transiently offer higher stability or lower end-to-end delay, the stack biases decisions toward the LEO backhaul, exploiting wide-area coverage and predictable geometry. This adaptivity suits heterogeneous missions where requirements vary over time and a network-level optimum (not a myopic per-hop choice) is preferred. Our contribution is not a new protocol but a pluggable CCM with reference integrations in OLSR and AODV for hybrid NTN deployments. Implementation is via a software shim that hooks the metric interface without altering base state machines or timers. Required telemetry (residual energy normalized to $[0, 1]$, link/path-loss in dB, optional timestamp) is conveyed in a TLV (Type–Length–Value) piggy-backed on existing control messages—HELLO/TC for OLSR and RREQ/RREP for AODV. The TLV uses a private type code and compact encoding; legacy nodes ignore unknown TLVs and continue with their baseline metric, preserving backward compatibility in mixed fleets. CCM-capable nodes parse the TLV, update per-neighbor state, and apply CCM at next-hop/route selection. No base headers are repurposed, checksums remain valid, and an optional capability bit can advertise CCM support.

The CCM and its associated protocols are designed to adapt to rapid network topology and node state changes. In AODV-CCM, the on-demand nature of route discovery ensures that the most current link and energy state information is used when establishing a new route. In OLSR-CCM, the periodic exchange of HELLO and TC messages, now augmented with CCM data, allows the network to continuously adapt to changes, although there is a risk of routing update delays if the update interval is not tuned to the mobility speed. Future work could explore dynamically adjusting the update interval based on network volatility. While we focus on residual energy, the CCM framework is extensible; other energy management strategies, such as incorporating energy consumption rate or prioritizing nodes with more stable energy sources, could be integrated by adding new terms to the metric. This would allow for even more nuanced and context-aware routing decisions.

1) *The Composite Cost Metric*: We define a Composite Cost Metric to balance link attenuation and node battery constraints in path selection. Although we primarily focus on the more significant losses between UAVs and LEO satellites, we also include inter-UAV link losses (which are typically smaller or practically negligible comparatively) for completeness. Let n denote the total number of *links* (or hops) in a candidate end-to-end route. For each link $i \in \{1, \dots, n\}$, we first calculate its free space path loss $FSPL_i$ in decibels (dB) using (6) and we subsequently proceed with the summation of these dB values is a convenient way to represent total path attenuation:

$$FSPL_{\text{path}}(\text{dB}) = \sum_{i=1}^n FSPL_i(\text{dB}). \quad (7)$$

To ensure dimensional consistency with energy-based metrics in our final cost function, we convert this *total* path loss from

dB into the factor:

$$L_{\text{path}} = 10^{\left(\text{FSPL}_{\text{path}}(\text{dB})/10\right)}. \quad (8)$$

Hence, rather than converting each link's loss to linear individually, we simply exponentiate the summed dB values once to obtain L_{path} .

Residual Energy: Next, we capture the average battery status of the *nodes* along this path (including ground relays or UAVs). Let E_i be the current residual energy of node i , and let $E_{i_{\text{max}}}$ denote its maximum energy capacity. To quantify how depleted or sustainable the route's relays are, we define

$$E_r = \frac{1}{n} \sum_{i=1}^n \left(\frac{E_i}{E_{i_{\text{max}}}} \right) \times 100\%, \quad (9)$$

which represents the *average residual energy fraction* (as a percentage) across the n nodes participating in the path.

Definition of CCM: Finally, we combine these two factors—path attenuation and residual energy fraction—into a cost metric:

$$\text{CCM} = \frac{L_{\text{path}}}{E_r}. \quad (10)$$

Here in Equation (10), L_{path} is the aggregate linear path-loss factor, and E_r is the percentage of residual energy. A high CCM indicates either large cumulative attenuation or low node energies (or both), making the path less desirable. Although FSPL does not inherently depend on energy, this formulation allows us to penalize routes that either have very poor signal quality or are likely to lose relaying nodes prematurely due to battery depletion. Since L_{path} is dimensionless (obtained from converting dB to linear scale) and E_r is also dimensionless (expressed as a percentage), CCM becomes a pure, dimensionless score for ranking candidate end-to-end routing paths. While no direct physical law couples path loss and node energy, combining them in one metric ensures that routing decisions avoid both high-attenuation links and severely depleted nodes, thereby improving overall network reliability.

A. Enhancing AODV with the CCM Metric

a) Message Structure Enhancement: The RREQ and RREP messages in AODV have been modified to accommodate the components of the CCM.

For the RREQ message, the original structure: [Type | Flags | Hop Count | RREQ ID | Destination IP | Destination Sequence | Origin IP | Origin Sequence] is expanded to include fields for FSPL and residual energy. This extension allows each node to compute and forward the FSPL and the residual energy of nodes along the proposed route. The enhanced RREQ structure is [Type | Flags | Hop Count | RREQ ID | Destination IP | Destination Sequence | Origin IP | Origin Sequence | FSPL | Avg Residual Energy]. The structure of the RREQ messages can be seen in Figure 3.

For the RREP message, the key enhancement is the inclusion of a field to carry back the aggregated CCM value of the route. The CCM is a crucial element for the route selection process, as it combines the FSPL and residual energy metrics

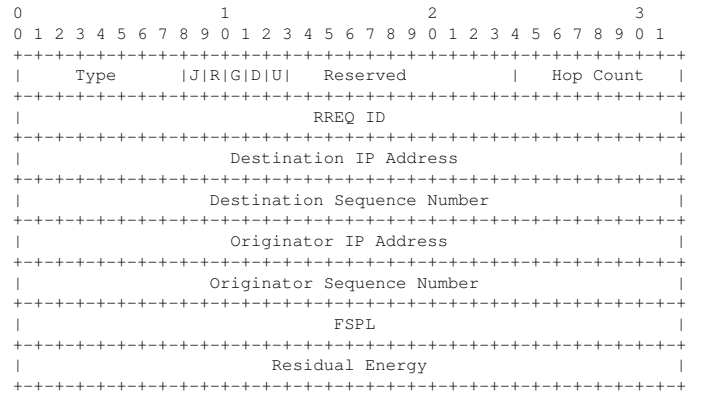


Figure 3: AODV-CCM Route Request (RREQ) Packet Structure

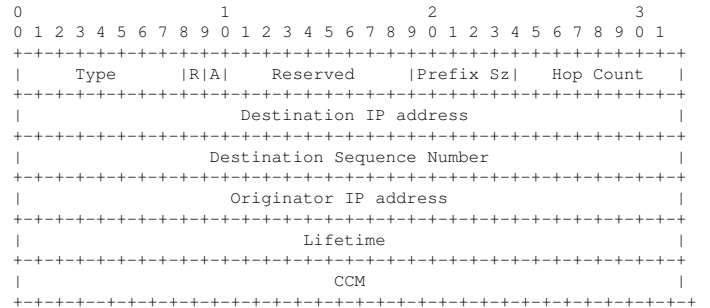


Figure 4: AODV-CCM Route Reply (RREP) Packet Structure

for the entire route. The revised RREP structure will include a field for the CCM value, resulting in [Type | Flags | Prefix Size | Hop Count | Destination IP | Destination Sequence Number | Origin IP | Lifetime | CCM]. The RREQ conveys individual link metrics (FSPL and energy) while the RREP carries the aggregate route CCM, allowing for more informed and efficient routing decisions. The structure of the RREP messages can be seen in Figure 4.

b) Route Calculation Mechanism and Packet Loss Model:

In our enhanced AODV protocol, which now incorporates the CCM, route selection is systematically guided by both link attenuation and node energy constraints. Figure 5 outlines the step-by-step process:

- 1) **Reception of RREQ:** The process begins when a node receives a RREQ message carrying two key parameters: (i) the cumulative FSPL along the path from the origin node to the current node, and (ii) the average residual energy of all intermediate nodes so far.
- 2) **Computation of CCM:** Upon receiving a RREQ, each node computes the CCM for the partial route from the source to itself. This calculation aggregates the total FSPL (as a proxy for link quality) and the average residual energy of the path's relays. Nodes with higher path loss or depleted batteries yield a higher CCM, indicating a less favorable route.
- 3) **Forwarding the RREQ:** If the node is not the final destination, it appends its own local FSPL and residual energy information and forwards the updated RREQ.

Consequently, subsequent nodes can recalculate the CCM with more complete path information.

- 4) **Generation of Route Reply (RREP):** When the RREQ reaches the destination or an intermediate node with a valid route, a RREP is generated. This message includes the final, aggregated CCM value for the entire path.
- 5) **Route Selection Based on CCM:** As RREP messages travel back toward the source, each intermediate node updates its routing table and prioritizes paths with the *lowest* CCM. This ensures that final route decisions favor energy-efficient, lower-attenuation paths.

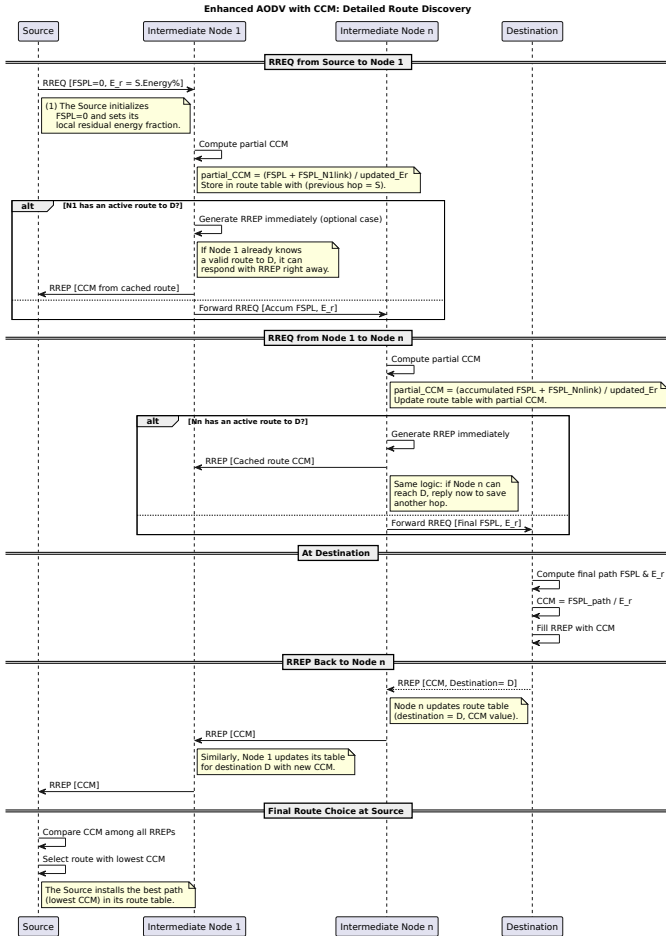


Figure 5: Sequence Diagram of the CCM-enhanced AODV route establishment process

While CCM employs FSPL as a surrogate for link quality, packet-loss events in our ns-3 simulations are determined by the underlying physical-layer error model, specifically the YansErrorRateModel. In this model, the receiver's signal-to-noise ratio (SNR) is calculated by subtracting the cumulative FSPL from the transmit power, incorporating additional attenuation factors such as fading. The error rate model then applies modulation-specific BER equations to probabilistically determine whether each incoming packet is successfully decoded or lost. Higher FSPL naturally results in lower SNR, thereby increasing the likelihood of packet drops. Consequently, CCM indirectly influences the packet delivery ratio (PDR): routes with excessive path loss incur

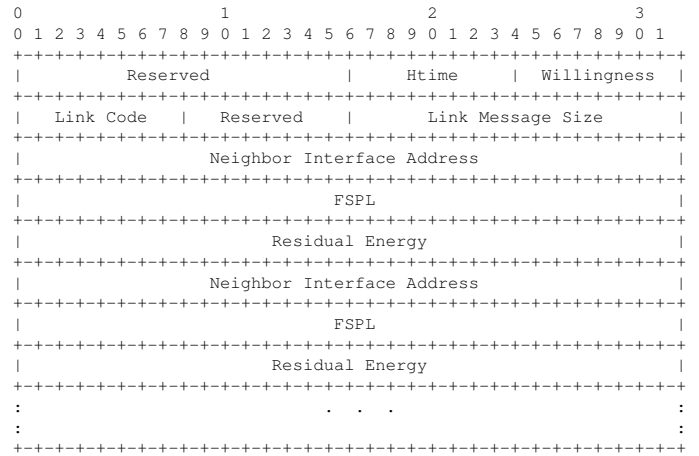


Figure 6: Enhanced OLSR HELLO Message Structure

higher packet losses, leading to larger CCM values and making them less likely to be selected. This approach mirrors the intent of metrics like ETX, which account for the average number of transmissions needed by considering packet loss probabilities.

By integrating the CCM into the AODV's route calculation mechanism, the protocol significantly enhances its ability to select the most efficient and stable paths. This approach not only optimizes network performance but also contributes to the longevity and sustainability of the network by prioritizing more efficient routes.

B. Enhancing OLSR with CCM-Mapped MPR Willingness

a) *Message Structure Enhancement in OLSR:* The OLSR protocol has been adapted to incorporate the components of the CCM, specifically the FSPL and residual energy metrics. This adaptation enhances the protocol's ability to make more informed decisions regarding route selection and Multi-Point Relay (MPR) selection. In the enhanced OLSR protocol, the Hello and Topology Control (TC) messages are modified to include FSPL and residual energy data.

For the Hello message, the original structure is expanded to include fields for FSPL and the node's residual energy. This extension enables nodes to broadcast their link quality (FSPL) and energy status to their immediate neighbors. The updated Hello message structure becomes [Type | VTime | Willingness | Link Code | Link Message Size | Neighbor Interface Address | FSPL | Residual Energy]. The structure of the new OLSR HELLO message can be seen in Figure 6.

For the TC message, similarly, the TC message is augmented to carry the FSPL and residual energy information of the MPRs. This information is used by other nodes in the network to calculate the CCM for routes passing through these MPRs. The revised TC message structure is [Type | ANSN | Reserved | Advertised Neighbor Main Address | FSPL | Residual Energy]. The structure of the TC message can be seen in Figure 7.

In this enhanced OLSR framework, each node calculates the CCM for its potential routes locally, based on the FSPL and residual energy information received from peers. This local

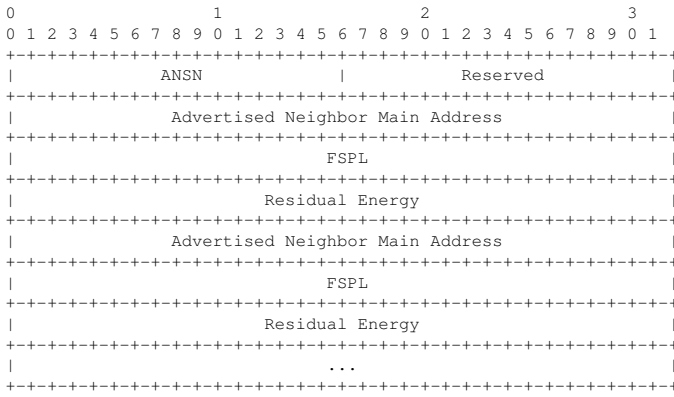


Figure 7: Enhanced OLSR TC Message Structure

calculation of CCM informs the node’s willingness to serve as an MPR, as well as its decision-making process when selecting MPRs for efficient route establishment. This approach ensures that route and MPR selection are grounded in the latest, most relevant data.

b) Route Calculation Mechanism: In the Enhanced OLSR protocol integrating the CCM, a sophisticated mechanism for dynamic willingness adjustment is employed. This mechanism is designed to respond to changes in the CCM, which reflects the cost-efficiency of potential routes. Figure 8 demonstrates the function of this mechanism, which is also described as:

- 1) Each OLSR node continuously monitors the CCM of potential routes. The CCM calculation is based on the cumulative FSPL for the entire path and the average residual energy of all nodes along that path.
- 2) If a node observes that the CCM of a potential route decreases in two (or more, depending on network policy) consecutive updates, this indicates an improvement in the route’s efficiency (either through reduced path loss or increased residual energy). In response, the node increases its willingness to become a Multi-Point Relay (MPR) by 1 point. This increment in willingness signifies a higher propensity to participate in routing due to the improved route quality. Conversely, if the CCM increases in one or two consecutive updates (again, based on network policy), this signals a decline in the route’s efficiency. The node will then decrease its willingness to serve as an MPR, reflecting the less favorable conditions for routing.
- 3) This adjustment mechanism is carefully balanced to ensure responsiveness to changes in network conditions while avoiding excessive fluctuations in willingness. A node only changes its willingness after observing consistent trends in the CCM, thereby ensuring that transient or minor variations in network conditions do not lead to abrupt changes in routing behavior.
- 4) Impact on MPR Selection and Routing: These dynamic adjustments in willingness directly influence MPR selection. Nodes with increased willingness are more likely to be chosen as MPRs, thus promoting the use of more efficient routes. Conversely, nodes with decreased willingness are less likely to be selected, steering the network

away from less efficient paths.

This approach to willingness adjustment for relay selection allows the network to continuously adapt to changing conditions, optimizing routing decisions for both energy efficiency and link stability. Dynamic willingness adjustment makes OLSR highly adaptive, ensuring that the network’s routing decisions are better aligned with the current optimal conditions, leading to improved overall performance - albeit some additional control overhead.

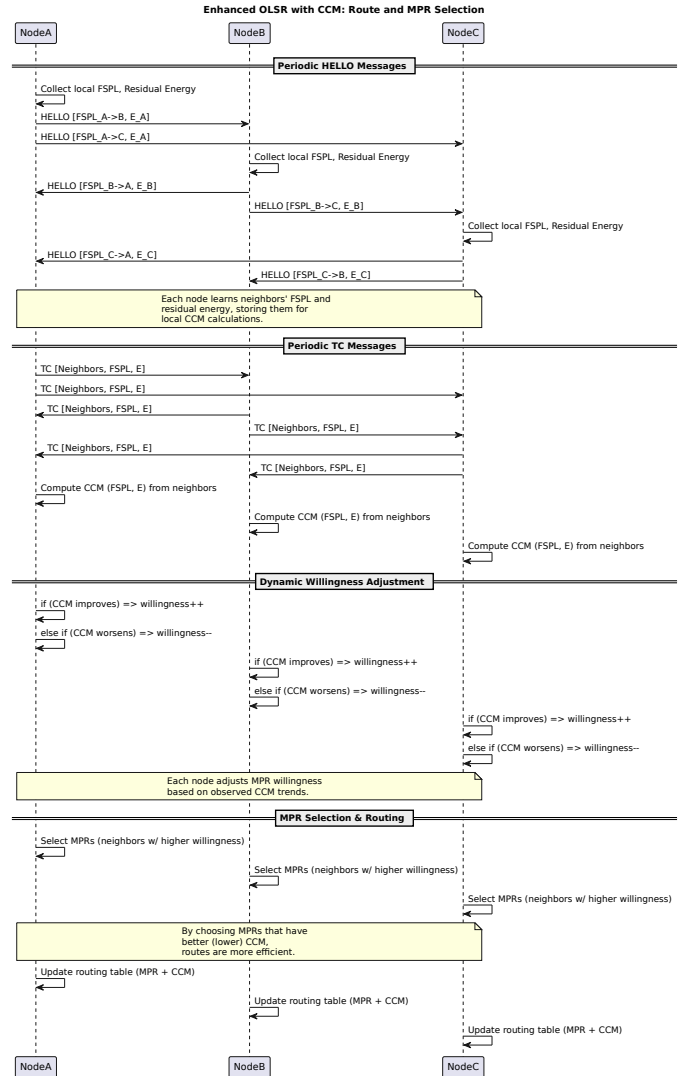


Figure 8: Sequence Diagram of the CCM-enhanced OLSR route establishment process

The added complexity of calculating and mapping CCM to willingness in this almost congestion window-like manner, must be offset by significant performance improvements. The research must demonstrate that the benefits in network performance justify the increased complexity. The dynamic nature of CCM-mapped willingness may lead to more frequent changes in MPR structure. Algorithms must ensure that these changes don’t lead to instability or excessive control traffic. Considerations will be made regarding the practical implementation of such a system, including computational

limitations and the potential need for additional resources. By integrating CCM into AODV and OLSR protocols, we aim to ensure that routes are selected in a manner that truly reflects the multidimensional nature of network performance and operational objectives.

V. EVALUATION

To validate our methodology, we conducted Monte Carlo simulations on the NS-3 platform, executing 20 individual runs for each scenario to ensure statistical reliability. The results presented are averaged over these runs to provide robust performance metrics. Our simulation framework includes two additional routing protocols for comparison, namely AOMDV and the Cyber-Physical Routing protocol [6], to provide a comprehensive performance evaluation against different routing paradigms. We integrated real-world data from existing the Starlink LEO constellation and compared the performance of our modified protocols against these standard and advanced implementations under various network conditions. Table I summarizes the utilized simulation parameters. Aerial ad hoc nodes are deployed to execute cellular communication relaying by leveraging the a 3D Gauss-Markov mobility model introduced in [25]. For readability and space efficiency, all multi-scenario figures are presented as vertically stacked subplots with legends placed inside each subplot; the legends explicitly include the mobility scenario tags (e.g., "UAV: 3DGM, UE: Static" and "UAV: RW3D, UE: RW2D").

In regards to the energy model, we employed a sophisticated energy consumption model to accurately simulate the operational dynamics of UAVs and Satellites within ns-3. The foundation of our energy model leverages ns-3's core classes (`LiIonEnergySource` for UAVs and `SimpleDeviceEnergyModel`), to represent the battery-powered characteristics of the nodes. To enhance the energy management capabilities for Satellites, we have developed a custom class, which inherits from the core class `ns3::LiIonEnergySource` and `ns3::SimpleDeviceEnergyModel`. This composite model integrates the standard energy source with an energy harvesting mechanism, enabling battery replenishment via solar panels, as it would be in a LEO orbit (we assume the same orbital parameters as those of the Starlink constellation: 550 km altitude). The custom class, which we named `CompositeEnergySource`, is available in a public repository. The energy model is available in our respective GitHub repository [26].

a) Energy Consumption per Delivered Packet vs Offered Load: Figure 9 shows the energy efficiency of routing protocols under two mobility scenarios using vertically stacked subplots. The top subplot shows performance under predictable mobility (UAV: 3D Gauss-Markov, UE: Static), where the CPR-TD protocol demonstrates good energy efficiency due to its ability to predict stable routes and minimize control overhead. The bottom subplot shows performance under volatile mobility (UAV: Random Walk 3D, UE: Random Walk 2D), where CPR-TD's energy consumption increases significantly as unpredictable movements lead to frequent link

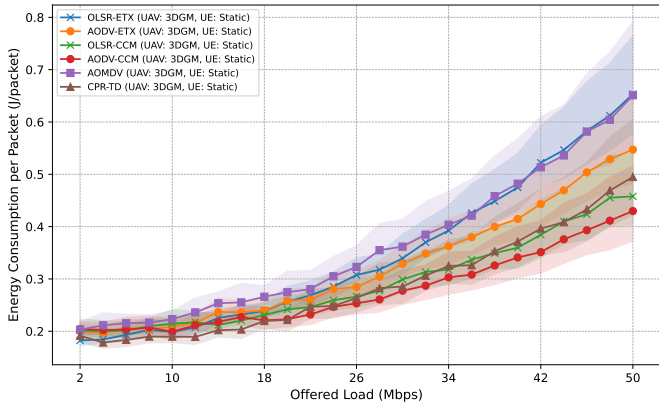
Table I: NS-3 Simulation Environment Parameters

Parameter	Description/Value
NS-3 Version	3.30
Modules Used	ns3-leo, aodv-etx, olsr-etx, aodv-ccm, olsr-ccm, aomdv, cpr-td
Network Size	UEs: 10-50, UAVs: 30, Satellites: 15
Altitude	UAVs: 300 m, Satellites: 550 km
MAC Standards	CSMA/CA-based
Propagation Model	Friis Free Space Path Loss Model
Frequency Band	1.8 GHz
Simulation Time	120 seconds
Simulation Area	5-25 km ² per interconnected cluster/ad hoc cell
Mobility Model	Users: Random Walk, UAVs: Anchored Self-Similar 3D Gauss-Markov, Satellites: LEO Circular-Orbit (Starlink constellation)
Traffic Type	UDP
Routing Protocols	AODV-ETX, OLSR-ETX AODV-CCM, OLSR-CCM AOMDV, CPR-TD
Energy Model	<code>LiIonEnergySource</code> (UAVs), <code>CompositeEnergySource</code> (Satellites)
Energy Consumption Rates	Tx: 2.33 A (UAVs), 4.66 A (Satellites) Rx: 1.5 A (UAVs), 3.0 A (Satellites) Idle: 1e-3 A

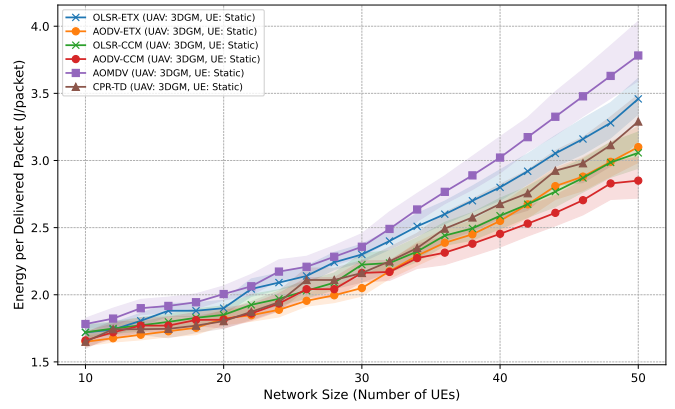
breaks, causing wasted energy on failed transmissions and route rediscoveries. The CCM-enhanced protocols maintain consistent energy efficiency across both scenarios. At low loads, the CCM variants (OLSR-CCM and AODV-CCM) incur a modest overhead because additional information embedded in control packets. This extra payload increases the energy cost per packet slightly. However, at higher loads, the benefit of improved route stability—stemming from CCM's ability to select energy-sustainable and lower-attenuation paths—outweighs the overhead. In AODV-CCM, for example, replacing the ETX metric with a composite cost that aggregates FSPL and node energy results in fewer route rediscoveries and retransmissions. Similarly, in OLSR-CCM, the dynamic mapping of CCM to the willingness parameter improves MPR selection, leading to fewer control message retransmissions. Nonetheless, one must note that in scenarios with very light traffic, the additional control overhead may temporarily render the CCM variants less energy-efficient than conventional implementations. The number of UEs is fixed to 50.

Across the $n = 20$ Monte Carlo runs, the $\pm 1\sigma$ bands widen with offered load; from mid-to-high loads the CCM variants remain separated from non-CCM baselines by about $\approx 1\sigma$, supporting a robust energy advantage, whereas at very low loads interval overlap indicates no material difference.

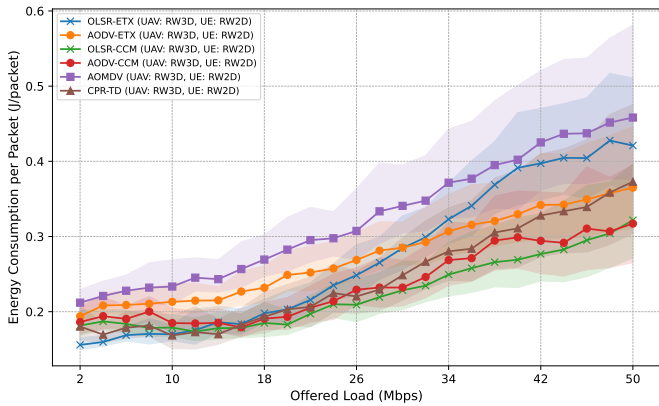
b) Energy Consumption vs Network Size: Figure 10 indicates that overall energy consumption increases with network size, but CCM-enabled protocols exhibit improved efficiency in denser networks. Similarly to the previous observation, at lower node densities, the extra control overhead introduced by CCM (via larger HELLO and TC messages) slightly elevates energy consumption. In denser networks, however, the benefits become more pronounced; the CCM metric's ability to balance load and select routes with extended lifetimes helps mitigate the exponential increase in energy expenditure that typically accompanies higher node counts. In effect, the additional overhead is amortized across many nodes and links, leading to an overall reduced energy footprint per delivered packet. Nonetheless, if the network density remains very low, the energy cost of transmitting the enhanced control packets might not be offset by the gains in route stability, causing CCM to underperform relative to simpler metrics. Offered load is fixed



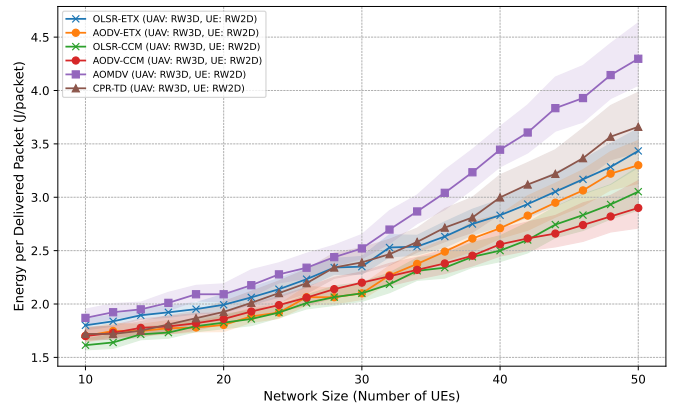
(a) Energy Consumption per Packet vs Offered Load (Mean $\pm 1\sigma$, $n = 20$) — UAV: 3DGM, UE: Static



(a) Energy per Delivered Packet vs Network Size (Mean $\pm 1\sigma$, $n = 20$) — UAV: 3DGM, UE: Static



(b) Energy Consumption per Packet vs Offered Load (Mean $\pm 1\sigma$, $n = 20$) — UAV: RW3D, UE: RW2D



(b) Energy per Delivered Packet vs Network Size (Mean $\pm 1\sigma$, $n = 20$) — UAV: RW3D, UE: RW2D

Figure 9: Energy Consumption per Delivered Packet vs Offered Load

Figure 10: Consumed energy vs Network Size

to 50 Mbps.

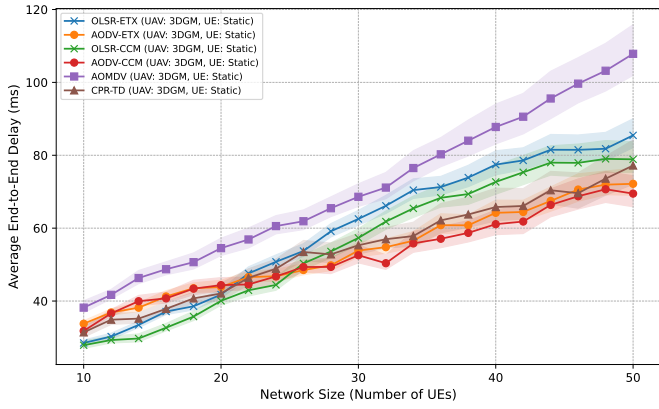
Uncertainty ($\pm 1\sigma$) grows with network size; in moderate-to-dense regimes the CCM curves are largely non-overlapping with baselines at roughly $\geq 1\sigma$ separation, supporting the efficiency gains, while at low densities substantial overlap suggests differences are not statistically pronounced.

c) *Average End-to-End Delay vs. Number of Nodes:* We consider e2e delay as the total time a data packet takes to travel from the source node to the destination node, encompassing all transmission, propagation, and processing delays at each intermediate hop. In our ns-3 simulations, this is measured in milliseconds (ms) using ns-3's built-in tracing mechanisms, which capture the exact timestamps when a packet is sent and received. Figure 11 reveals that end-to-end delay is strongly influenced by network size and the inherent protocol mechanics. In low-density networks, proactive routing (as in OLSR) yields lower delays because the network topology is maintained continuously. However, as density increases, the reactive nature of AODV-based protocols starts to offer lower delays. AODV-CCM benefits from real-time FSPL and energy data, leading to more robust route selections that reduce packet retransmissions. On the other hand, the additional processing time required to compute the CCM—and the resulting increase

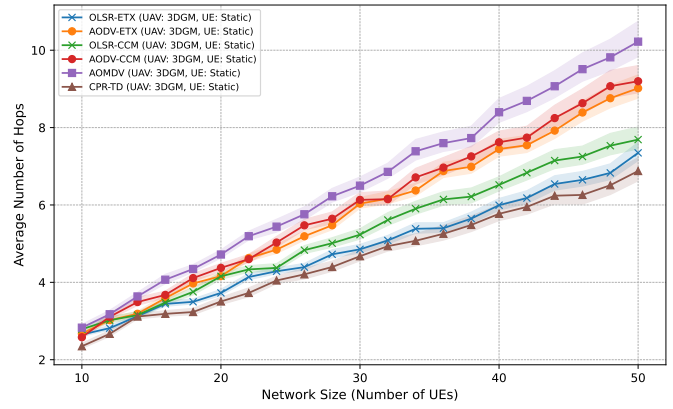
in control message size—introduces marginal delays, especially in OLSR-CCM where dynamic willingness adjustments may momentarily delay MPR re-selection. In environments where processing resources are limited or control overhead is significant, these delays might slightly negate the benefits provided by the CCM. Offered load is fixed to 50 Mbps.

Delay variability increases with node count; beyond about 30 UEs, AODV-CCM bands sit below AOMDV/OLSR-ETX by roughly $\approx 1\sigma$ in the static case and near 1σ in the volatile case, indicating a meaningful latency benefit, whereas for small networks the intervals overlap.

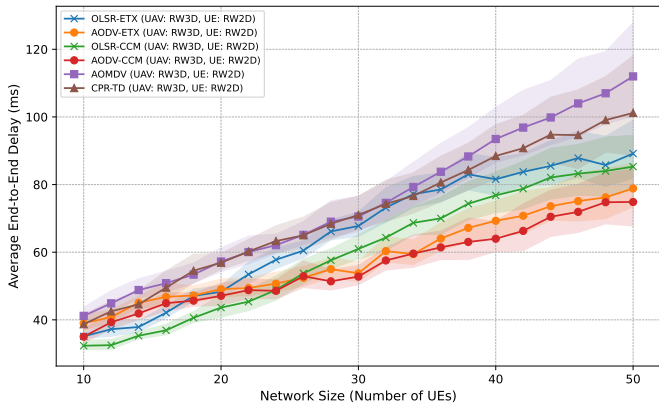
d) *Number of Hops vs. Network Size:* This graph examines how the average number of hops required for end-to-end communication changes as the network size increases. The X-axis represents network size—reflected in our simulations by an expanding deployment area (or an increasing UE count)—while the Y-axis shows the corresponding average hop count. In emergency scenarios, larger areas are necessary to cover regions where traditional infrastructure may be compromised. Although UEs do not act as relays in our considered network typologies, the expanded area forces data to traverse longer distances via dedicated relay nodes (such as UAVs and satellites), thereby increasing the hop count. The routing protocols differ in their design priorities: proactive protocols



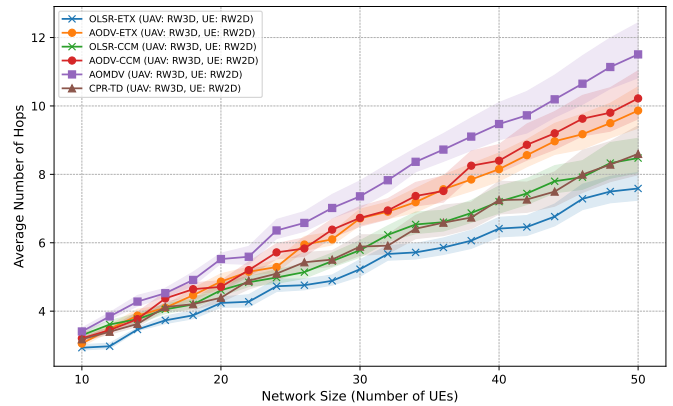
(a) Average End-to-End Delay vs Network Size (Mean $\pm 1\sigma$, $n = 20$) — UAV: 3DGM, UE: Static



(a) Number of Hops vs Network Size (Mean $\pm 1\sigma$, $n = 20$) — UAV: 3DGM, UE: Static



(b) Average End-to-End Delay vs Network Size (Mean $\pm 1\sigma$, $n = 20$) — UAV: RW3D, UE: RW2D



(b) Number of Hops vs Network Size (Mean $\pm 1\sigma$, $n = 20$) — UAV: RW3D, UE: RW2D

Figure 11: End-to-end Delay vs Network Size

Figure 12: Number of Hops vs Network Size

like OLSR generally yield shorter paths. This is particularly highlighted in the cast of CPR-TD which computes routes based on future node trajectory. Energy-aware variants like OLSR-CCM and AODV-CCM may intentionally select routes with additional hops to optimize energy distribution and link reliability; while reactive protocols such as AODV-ETX strike a balance by prioritizing link quality. This trade-off means that as network size increases, longer routes—though potentially more energy-efficient overall—can lead to higher hop counts, as illustrated in Figure 12. In practice, we observed a de-prioritization of UAV-LEO Satellite links, instead favoring inter-UAV relaying.

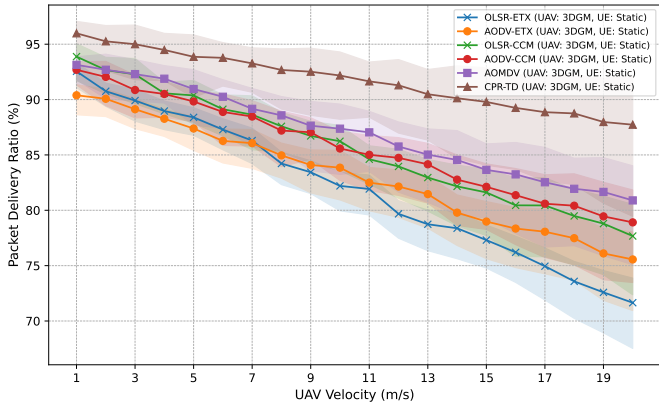
The hop-count variance grows mildly with density; CCM variants show slightly higher means but with overlapping $\pm 1\sigma$ envelopes against baselines, implying the hop increase is modest relative to variability and reflects energy-aware path choices rather than instability.

e) Packet Delivery Ratio vs. UAV Velocity: Figure 13 demonstrates the performance of routing protocols under two mobility scenarios using vertically stacked subplots. The top subplot shows performance under predictable mobility (UAV: 3D Gauss-Markov, UE: Static), where cyber-physical routing (as implemented in CPR-TD) excels due to its ability to predict smooth trajectories and maintain stable routes. The

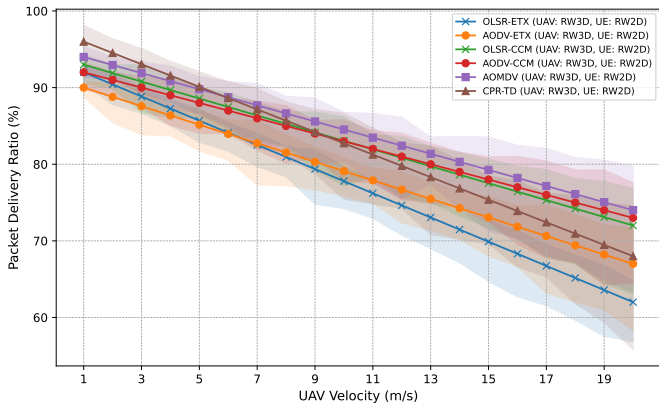
bottom subplot shows performance under volatile mobility (UAV: Random Walk 3D, UE: Random Walk 2D), where CPR-TD's performance degrades significantly as it cannot predict erratic movements, leading to frequent link breaks and packet loss. In contrast, CCM-enhanced protocols maintain consistent performance across both scenarios due to their real-time adaptation capabilities. AODV-CCM leverages real-time FSPL and energy information to quickly discard unstable routes, while OLSR-CCM benefits from enhanced MPR selection that adapts to current network conditions rather than relying on predictions. The multipath nature of AOMDV provides some resilience against volatility, but at the cost of higher control overhead. The X-axis represents UAV velocity, which affects both scenarios differently: in the 3D Gauss-Markov scenario, only UAVs move; in the Random Walk scenario, both UAVs and UEs contribute to the overall mobility. Offered load is fixed to 50 Mbps.

Uncertainty widens with velocity; under predictable mobility, CPR-TD exceeds others by more than 1σ over much of the range, whereas under volatile mobility CPR-TD falls below CCM with limited overlap at high speeds, evidencing robust degradation under volatility and the resilience of CCM.

f) Throughput vs Offered Load: Figure 14 illustrates the throughput performance under two mobility scenarios using



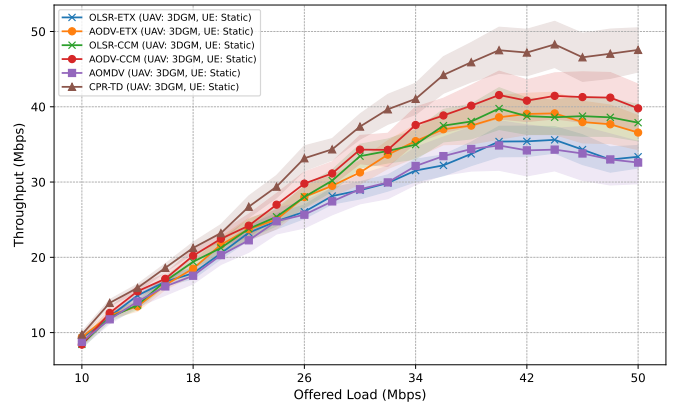
(a) Packet Delivery Ratio vs Node Mobility (Mean $\pm 1\sigma$, $n = 20$) — UAV: 3DGM, UE: Static



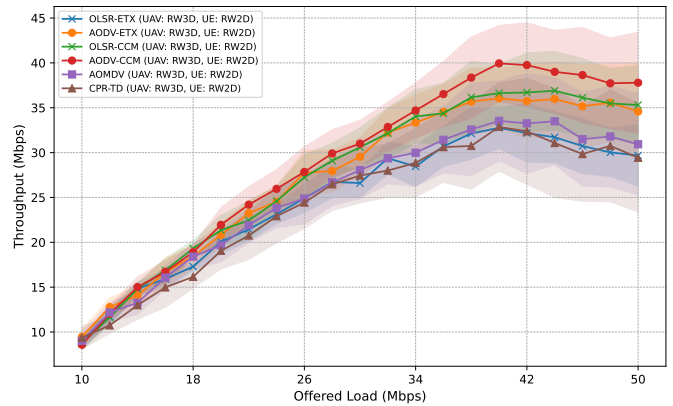
(b) Packet Delivery Ratio vs Node Mobility (Mean $\pm 1\sigma$, $n = 20$) — UAV: RW3D, UE: RW2D

Figure 13: Packet Delivery Ratio vs Node Mobility

vertically stacked subplots. The top subplot shows performance under predictable mobility (UAV: 3D Gauss-Markov, UE: Static), where CPR-TD achieves high throughput due to its efficient predictive routing. The bottom subplot shows performance under volatile mobility (UAV: Random Walk 3D, UE: Random Walk 2D), where CPR-TD's throughput significantly drops as it struggles with unpredictable link changes, leading to increased packet loss and retransmissions. CCM-enhanced protocols, particularly AODV-CCM, demonstrate more stable throughput across both scenarios due to their real-time adaptation to link quality and energy status, which minimizes the impact of sudden topology changes. While AOMDV provides some resilience through multipath routing, its inherent overhead can limit peak throughput, compared to CCM-enhanced protocols in certain conditions., with nuanced effects from the integration of CCM. AODV's on-demand nature inherently minimizes control traffic, leading to superior throughput at higher loads. The CCM enhances route stability by favoring paths with lower cumulative FSPL and higher residual energy, which reduces packet losses and retransmissions. In OLSR-CCM, mapping CCM to the willingness parameter improves MPR selection, which translates to better throughput despite the increased control overhead. However, the extra fields in control messages and the additional compu-



(a) Throughput vs Offered Load (Mean $\pm 1\sigma$, $n = 20$) — UAV: 3DGM, UE: Static



(b) Throughput vs Offered Load (Mean $\pm 1\sigma$, $n = 20$) — UAV: RW3D, UE: RW2D

Figure 14: Throughput vs Offered Load

tation required for CCM can introduce slight delays in route establishment. Interestingly, the delays are more noticeable under low offered loads, where the overhead might slightly reduce throughput compared to conventional metrics. Overall, while the CCM tends to deliver long-term throughput gains by ensuring more reliable routes, its benefits may be partially offset in scenarios where control overhead dominates the network load.

Across $n = 20$ runs, throughput variability increases with load; in static mobility AODV-CCM is separated from OLSR-ETX/AOMDV by roughly $\approx 1\sigma$ near saturation, while in volatile mobility both CCM variants retain an advantage with limited interval overlap, supporting the stability argument.

From a statistical standpoint across all figures, the shaded regions denote mean $\pm 1\sigma$ over $n = 20$ Monte Carlo runs. In the primary operating regimes for NTN (moderate to high offered load/network size and under volatile mobility), CCM-enhanced protocols maintain $\approx 1\sigma$ or greater separation from non-CCM baselines, indicating robust, repeatable gains; this is expected, as CCM explicitly biases route selection toward lower cumulative FSPL and higher residual energy, reducing retransmissions and route churn. Interval overlap mainly appears in low-load/low-density regimes where overhead dominates and benefits have little room to manifest.

VI. COMPLEXITY AND SCALABILITY ANALYSIS

The integration of the composite cost metric into routing protocols introduces additional computational, messaging, and memory overhead, which must be analyzed to understand its scalability in large-scale networks. This section examines the complexity of CCM-enhanced protocols in contrast to their baseline counterparts.

A. Algorithmic Complexity

The primary algorithmic overhead of our proposed enhancement lies in the calculation of the CCM itself and its integration into the decision-making processes of AODV and OLSR.

a) AODV-CCM: In AODV-ETX, the path cost is the cumulative ETX, an additive metric. Similarly, AODV-CCM requires accumulating FSPL and residual energy values during the RREQ dissemination. For a path with D hops, the CCM calculation involves approximately D additions and a single division. The per-node complexity for processing an RREQ is dominated by routing table lookups, which, using a hash table, is an $O(1)$ operation on average. When a node receives an RREQ, it updates the cumulative CCM values, which is an $O(D)$ operation. Given that the RREQ propagates through at most N nodes in a network of size N , the overall complexity of a single route discovery is $O(N \cdot D_{avg})$, where D_{avg} is the average path length. This is comparable to AODV-ETX.

b) OLSR-CCM: In OLSR, each node must periodically compute its MPR set. The complexity of the standard MPR selection algorithm is known to be NP-hard, though heuristics are used in practice. Our enhancement modifies the *willingness* parameter based on the CCM. The calculation of CCM for all neighbors adds a complexity of $O(|\mathcal{N}(s)|)$ for each node s , where $|\mathcal{N}(s)|$ is the number of neighbors. This calculation is performed periodically with HELLO messages. The subsequent path calculations using Dijkstra's algorithm have a complexity of $O(N \log N + E)$, where E is the number of edges. Since the CCM-based willingness might lead to more frequent topology updates if not tuned properly, the practical overhead could increase, though our simulations show this is manageable.

B. Message and Memory Complexity

The scalability of a routing protocol is heavily influenced by its control message overhead and the memory required to store routing information.

a) Message Overhead: Integrating CCM requires adding FSPL and residual energy fields to control packets.

- **AODV-CCM:** The RREQ packet is enlarged to carry cumulative FSPL and average residual energy (e.g., two 32-bit floating-point numbers), and the RREP carries the final CCM value. This adds a constant number of bytes to each control packet, resulting in a marginal increase in overhead per route discovery.
- **OLSR-CCM:** HELLO and TC messages are expanded. For each neighbor listed in a HELLO or TC message, FSPL and energy information must be included. If a node

has $|\mathcal{N}(s)|$ neighbors, the size of its HELLO message increases by $O(|\mathcal{N}(s)|)$. This can become significant in dense networks, as shown in our energy consumption analysis for low-density scenarios.

While the per-packet overhead increases, the enhanced route stability provided by CCM can lead to a reduction in the *total* number of control packets, as fewer route failures mean fewer RERR messages (in AODV) and potentially more stable MPR sets (in OLSR).

b) Memory Overhead: The memory complexity is primarily determined by the size of the routing tables.

- In **AODV-CCM**, each routing table entry must be augmented to store the CCM value for the path, in addition to the standard fields. This is a constant increase per entry, leading to an overall memory overhead of $O(N)$ for a node storing routes to all other nodes in the worst case.
- In **OLSR-CCM**, nodes maintain topology information for the entire network. The CCM enhancement requires storing FSPL and energy data for each link in the topology table. The size of the topology table is on the order of $O(N \cdot |\text{MPR_selectors}|)$, where $|\text{MPR_selectors}|$ is the number of nodes that have selected a given node as an MPR.

Compared to baseline protocols, the memory overhead of CCM is a linear increase with the size of the network, which is generally acceptable for the considered scenarios. The scalability is thus comparable to that of other state-of-the-art MANET protocols.

VII. LIMITATIONS AND APPLICABILITY

While the CCM offers significant advantages in terms of energy efficiency and route stability, it is essential to acknowledge its limitations and define the scenarios where it is most applicable. This section provides a critical discussion of these aspects.

a) Dependence on FSPL: The CCM currently relies on the FSPL model as a proxy for link quality. While FSPL is a fundamental component of path loss, it does not account for more complex propagation effects such as multipath fading, shadowing, or atmospheric absorption, which can be significant, especially for UAV-to-ground and satellite links. In environments with significant obstructions or complex terrain, the accuracy of the CCM could be diminished, potentially leading to suboptimal route selection. The framework is, however, extensible to incorporate more sophisticated channel models, though this would increase computational complexity.

b) Control Overhead in Low-Density or Low-Load Scenarios: As demonstrated in our simulation results, the additional control overhead introduced by the CCM can, in certain situations, outweigh its benefits. In sparse networks or under very light traffic loads, the energy consumed by the larger control packets of OLSR-CCM and the route discovery overhead of AODV-CCM may exceed the energy saved through more stable routes. Therefore, the CCM is most beneficial in moderately to densely populated networks with sufficient traffic to amortize the control overhead.

c) *Tuning of CCM Parameters:* The formulation of the CCM involves a direct trade-off between path loss and residual energy. While we have used a simple ratio, the relative importance of these two components may vary depending on the specific application or operational context. For instance, in a mission where network longevity is paramount, residual energy should be weighted more heavily. The current model does not include adaptive weighting, which could be a valuable extension for future work.

d) *Applicability in Homogeneous vs. Heterogeneous Networks:* The CCM is designed for heterogeneous networks comprising nodes with different energy constraints (e.g., battery-powered UAVs and solar-powered satellites). It is in these scenarios that the metric provides the most significant benefit, by preventing the premature failure of energy-constrained nodes. In more homogeneous networks where all nodes have similar energy profiles, the benefits of the energy-aware component of the CCM would be less pronounced, and simpler link-quality metrics like ETX might offer comparable performance with lower overhead.

e) *Scalability Concerns in Very Large Networks:* While our analysis shows that the complexity of CCM is manageable for the scenarios considered, its scalability in extremely large-scale networks (e.g., mega-constellations with thousands of satellites) has not been tested. The message overhead of OLSR-CCM, in particular, could become a limiting factor. Hierarchical routing schemes or more advanced MPR selection strategies might be necessary to apply CCM effectively in such environments.

VIII. PRACTICAL DEPLOYMENT CONSIDERATIONS

Deploying the CCM-enhanced routing protocols in a real-world hybrid UAV-satellite NTN requires careful consideration of several practical aspects, from software modifications to network management.

a) *Implementation as a Software Update:* A key advantage of our approach is that it is a distributed scheme that can be implemented as a software update to existing routing stacks on UAVs and satellite nodes. No specialized hardware is required. The modifications are confined to the network layer, specifically the routing agent. This makes the CCM an attractive option for retrofitting existing systems, as it does not necessitate large-scale changes to network infrastructure. The primary requirement is that nodes must have a mechanism to estimate their own residual energy and to calculate the distance to their neighbors (e.g., via GPS).

b) *Distributed Nature:* The CCM-enhanced protocols operate in a fully distributed manner. Each node makes its own routing decisions based on locally available information and the information exchanged with its neighbors. There is no central controller, which makes the system robust and resilient to single points of failure—a critical feature for mission-critical applications in disaster-stricken or remote areas.

c) *Interoperability:* When deploying CCM-enhanced protocols, interoperability with nodes that do not support the CCM is a concern. A hybrid network could operate in a mixed mode, where CCM-enabled nodes can take advantage

of the enhanced metric when communicating with each other, but would revert to a baseline metric (e.g., hop count or ETX) when communicating with non-CCM nodes. This would require careful handling of the metric fields in control packets to ensure backward compatibility.

d) *Energy Measurement Accuracy:* The effectiveness of the CCM is contingent on the ability of nodes to accurately report their residual energy. For battery-powered UAVs, this requires a well-calibrated battery management system (BMS). For solar-powered satellites, the energy model must account for the efficiency of the solar panels and the state of the battery. Inaccurate energy reporting could lead to skewed CCM calculations and suboptimal routing decisions.

e) *Security Considerations:* The introduction of new fields in routing packets could potentially open new vectors for security attacks. For example, a malicious node could advertise a very high residual energy to attract traffic, thereby launching a blackhole or grayhole attack. Therefore, the deployment of CCM-enhanced protocols should be accompanied by appropriate security mechanisms, such as message authentication, to ensure the integrity of the routing information.

IX. CONCLUSIONS

This paper introduced a composite cost metric to enhance energy-efficient routing in hybrid UAV-satellite NTNs for 6G. By integrating cumulative FSPL and residual energy, we developed a metric that can be embedded into both proactive (OLSR) and reactive (AODV) routing protocols. Our NS-3 simulation framework, which includes realistic mobility and a novel composite energy model, demonstrates that CCM-enhanced protocols improve energy efficiency and packet delivery ratios, particularly under high network load and density, at the cost of some control overhead. This work paves the way for more robust, reliable, and energy-aware routing solutions for mission-critical communications in future NTN-supported 6G networks. Future work will focus on adaptive control strategies, machine learning-based predictive routing, and expanding the simulation framework to include a wider range of satellite constellation parameters.

REFERENCES

- [1] B. Li, Z. Li, H. Zhou, X. Chen, Y. Peng, P. Yu, Y. Wang, and X. Feng, "A System of Power Emergency Communication System Based BDS and LEO Satellite," in *2021 Computing, Communications and IoT Applications (ComComAp)*, 2021, pp. 286–291.
- [2] M. M. Saad, M. A. Tariq, M. T. R. Khan, and D. Kim, "Non-Terrestrial Networks: An Overview of 3GPP Release 17 & 18," *IEEE Internet of Things Magazine*, vol. 7, no. 1, pp. 20–26, 2024.
- [3] D. S. Lakew, A.-T. Tran, N.-N. Dao, and S. Cho, "Intelligent Self-Optimization for Task Offloading in LEO-MEC-Assisted Energy-Harvesting-UAV Systems," *IEEE Transactions on Network Science and Engineering*, pp. 1–14, 2024.
- [4] M. K. Marina and S. R. Das, "On-demand Multipath Distance Vector Routing in Ad Hoc Networks," in *Proceedings of the Ninth International Conference on Network Protocols (ICNP)*, 2001, pp. 14–23.
- [5] Y. Yuan, H. Chen, and M. Jia, "An Optimized Ad-hoc On-demand Multipath Distance Vector (AOMDV) Routing Protocol," in *2005 Asia-Pacific Conference on Communications*, Perth, WA, 2005, pp. 569–573.
- [6] D. Hu, S. Yang, M. Gong, Z. Feng, and X. Zhu, "A cyber-physical routing protocol exploiting trajectory dynamics for mission-oriented flying ad hoc networks," *Engineering*, vol. 19, no. 12, pp. 217–227, 2022.

- [7] D. Huo, Q. Liu, Y. Sun, and H. Li, "A Large Inter-satellite Non-dependent Routing Technology – IS-OLSR," in *2021 17th International Conference on Mobility, Sensing and Networking (MSN)*, 2021, pp. 25–31.
- [8] H. Liming, K. Shaoli, S. Shaohui, M. Deshan, H. Bo, and Z. Meiting, "A load balancing routing method based on real time traffic in LEO satellite constellation space networks," in *2022 IEEE 95th Vehicular Technology Conference: (VTC2022-Spring)*, 2022, pp. 1–5.
- [9] Z. Liu, Z. Liu, L. Wang, and W. Li, "Traffic-Predictive Routing Strategy for Satellite Networks," *Electronics*, vol. 13, no. 1, 2024.
- [10] S. Suhaimi, K. Mamat, and K. D. Wong, "Enhancing the "Willingness" on the OLSR Protocol: Methodology on Experimenting the Real Testbed," in *2009 5th International Conference on Wireless Communications, Networking and Mobile Computing*, 2009, pp. 1–4.
- [11] S. Jiao, C. Wang, R. Sun, Y. Wang, L. Jia, and J. Chen, "Routing Design and Experimental Validation on a Satellite 5G Bearer Network," in *2022 IEEE 8th International Conference on Computer and Communications (ICCC)*, 2022, pp. 638–643.
- [12] M.-H. T. Nguyen, T. T. Bui, L. D. Nguyen, E. Garcia-Palacios, H.-J. Zepernick, and T. Q. Duong, "Real-Time Large-Scale 6G Satellite-UAV Networks," in *2023 IEEE Statistical Signal Processing Workshop (SSP)*, Hanoi, Vietnam, 2023, pp. 100–104.
- [13] Y. Wang, W. Feng, J. Wang, and T. Q. S. Quek, "Hybrid Satellite-UAV-Terrestrial Networks for 6G Ubiquitous Coverage: A Maritime Communications Perspective," *IEEE Journal on Selected Areas in Communications*, vol. 39, no. 11, pp. 3475–3490, Nov 2021.
- [14] C. Liu, W. Feng, Y. Chen, C.-X. Wang, and N. Ge, "Cell-Free Satellite-UAV Networks for 6G Wide-Area Internet of Things," *IEEE Journal on Selected Areas in Communications*, vol. 39, no. 4, pp. 1116–1131, Apr 2021.
- [15] S. Zhang, H. Zhang, and L. Song, "Beyond D2D: Full Dimension UAV-to-Everything Communications in 6G," *IEEE Transactions on Vehicular Technology*, vol. 69, no. 6, pp. 6592–6602, Jun 2020.
- [16] Q. Wang, X. Chen, and Q. Qi, "Energy-Efficient Design of Satellite-Terrestrial Computing in 6G Wireless Networks," *IEEE Transactions on Communications*, vol. 72, no. 3, pp. 1759–1772, Mar 2024.
- [17] Z. Jia, C. Dong, K. Guo, and Q. Wu, "The Potential of LEO Satellites in 6G Space-Air-Ground Enabled Access Networks," 2023. [Online]. Available: [https://arxiv.org/abs/2307.00234]
- [18] W.-Y. Dong, S. Yang, and S. Chen, "Uplink performance analysis of heterogeneous non-terrestrial networks in harsh environments: A novel stochastic geometry model," *IEEE Transactions on Communications*, 2025, early access, Jan. 2025.
- [19] W.-Y. Dong, S. Yang, P. Zhang, and S. Chen, "Stochastic Geometry Based Modeling and Analysis of Uplink Cooperative Satellite-Aerial-Terrestrial Networks for Nomadic Communications With Weak Satellite Coverage," *IEEE Journal on Selected Areas in Communications*, vol. 42, no. 12, pp. 3428–3444, 2024.
- [20] S. Yang, W. Zhao, C.-M. Wang, W.-Y. Dong, and X. Ju, "Betweenness centrality based dynamic source routing for flying ad hoc networks in marching formation," *IEEE Transactions on Vehicular Technology*, 2025, early access, Mar. 2025.
- [21] C.-M. Wang, S. Yang, W.-Y. Dong, W. Zhao, and W. Lin, "A Distributed Hybrid Proactive-Reactive Ant Colony Routing Protocol for Highly Dynamic FANETs With Link Quality Prediction," *IEEE Transactions on Vehicular Technology*, vol. 74, no. 1, pp. 1817–1822, 2025.
- [22] D. S. J. De Couto, D. Aguayo, J. Bicket, and R. Morris, "A High-Throughput Path Metric for Multi-Hop Wireless Routing," *Wireless Networks*, vol. 11, pp. 419–434, Jul 2005.
- [23] T. Clausen and P. Jacquet, "Optimized Link State Routing Protocol (OLSR)," RFC 3626, IETF, RFC, Oct. 2003. [Online]. Available: [https://www.rfc-editor.org/info/rfc3626]
- [24] C. Perkins, E. Belding-Royer, and S. Das, "Ad hoc On-Demand Distance Vector (AODV) Routing," RFC 3561, IETF, RFC, Jul. 2003. [Online]. Available: [https://www.rfc-editor.org/info/rfc3561]
- [25] G. Amponis, T. Lagkas, V. Argyriou, I. Moscholios, M. Zevgara, S. Ouzounidis, and P. Sarigiannidis, "Anchored self-similar 3D Gauss-Markov mobility model for ad hoc routing scenarios," *IET Networks*, vol. 12, no. 5, pp. 250–259, 2023.
- [26] G. Amponis, "NS-3 Composite Energy Source Model," Software, 2025, implements a Li-Ion energy source with solar harvesting (LEO cycle and fixed window) for ns-3. [Online]. Available: [https://github.com/g-ampon/NS3-composite-energy-source-model]

George Amponis received his B.Sc. degree from the Department of Information and Electronic Engineering of the International Hellenic University, School of Engineering in 2020, and his PhD from the Department of Informatics of the Democritus University of Thrace, School of Natural Sciences in 2025. He has experience in ad hoc networking, embedded systems and firmware development for a wide range of applications. His research interests include wireless communications, routing protocols for drone swarms, security in 5G environments, secure real-time communications, link- and transport-layer protocols with an emphasis on congestion avoidance. He is a member of IEEE and has authored numerous publications in the field of routing, ad hoc networks and next generation cellular communications.

Dr. Thomas Lagkas is Assistant Professor at the Department of Computer Science of the Democritus University of Thrace and Director of the Laboratory of Industrial and Educational Embedded Systems. He graduated with honours from the Department of Informatics, Aristotle University of Thessaloniki and awarded PhD on Wireless Networks. He also completed MBA studies at the Hellenic Open University and received a postgraduate certificate on Teaching and Learning from The University of Sheffield. He has been scholar of the Aristotle University Research Committee and postdoctoral scholar of the National Scholarships Institute of Greece. His research interests are in the areas of IoT communications with numerous highly cited publications. Dr. Lagkas is an IEEE Senior Member, Fellow of the Higher Education Academy in the UK, and member of the Editorial Board of reputable scientific journals. Moreover, he actively participates in several EU-funded research projects.

Pavlos Bouzinis received the Diploma (five years) and Ph.D. degrees in electrical and computer engineering from the Aristotle University of Thessaloniki, Greece, in 2019 and 2023, respectively, where he was a member of the Wireless Communications and Information Processing Group. Currently, he works as a research engineer at MetaMind Innovations P.C. His main research interests include machine learning, optimization, and intrusion detection systems. He has served as a reviewer for several scientific journals and was an exemplary reviewer of IEEE WIRELESS COMMUNICATIONS LETTERS, in 2021 (top 3% of reviewers).

Dr. Panagiotis Radoglou-Grammatikis received Diploma (five years) and PhD from the Dept. of Electrical and Computer Engineering, University of Western Macedonia, Greece, in 2016 and 2023, respectively. His main research interests focus on AI-driven cybersecurity, intrusion detection and security games. He has published more than 50 research papers in international scientific journals, conferences and book chapters, while he has received five best paper awards. He was included in Stanford University's list (shared by Elsevier) of the Top 2% of Scientists in the World for 2021 and 2022. Currently, he is working as a research director at K3Y Ltd, while he is also a postdoc researcher at the ITHACA Lab of the University of Western Macedonia and co-founder of MetaMind Innovations P.C. He is involved in several national and international projects. Finally, he is a member of IEEE, ACM and the Technical Chamber of Greece.

Antonios Sarigiannidis received the B.Sc. degree in Information Technology from the Aristotle University of Thessaloniki in 2007 and the M.Sc. degree in Communication Systems and Technologies, specialising in advanced optical and wireless technologies, from the Aristotle University of Thessaloniki in 2009. He obtained his Ph.D. in Information Technology from the Aristotle University of Thessaloniki in 2016. His Ph.D. thesis includes the development of bandwidth allocation algorithms in Communication Networks. His research interests include machine learning mechanism and optimisation techniques as well as visualisation techniques regarding analytics, big data and security analysis. Recently, he has been involved in IoT and M2M research towards in coverage analysis and security services. He actively participated in both national and EU funded projects. He is the author of more than 30 publications in leading international journals and conferences.

Prof. Panagiotis Sarigiannidis is the Director of ITHACA Lab, Co-Founder of MetaMind Innovations P.C. and Full Professor at the Department of Electrical and Computer Engineering, University of Western Macedonia, Kozani, Greece. He received his B.Sc. and Ph.D. in computer science from the Aristotle University of Thessaloniki, Thessaloniki, Greece, in 2001 and 2007, respectively. His research interests include telecommunication networks, Internet of Things and cybersecurity. He has published over 270 papers in international journals, conferences and book chapters, while he has also received five best paper awards. He is involved in several national and international projects. He served as the project coordinator of three H2020 projects, namely SPEAR, EVIDENT and TERMINET. Moreover, he has coordinated national and Erasmus+ KA2 projects, while he served as a principal investigator in SDN-microSENSE and three Erasmus+ KA2: ARRANGE-ICT, JAUNTY and STRONG. Finally, he participates in several editorial boards of various journals.

Prof. Vasileios Argyriou received the B.Sc. degree in computer science from the Aristotle University of Thessaloniki, Greece, in 2001, and the M.Sc. and Ph.D. degrees in electrical engineering working on registration from the University of Surrey, in 2003 and 2006, respectively. From 2001 to 2002, he held a research position with Aristotle University, with a focus on image and video watermarking. He joined the Communications and Signal Processing Department, Imperial College London, London, in 2007, where he was a Research Fellow working on 3D object reconstruction. He is currently a Professor with Kingston University, London, working on computer vision and AI for crowd and human behavior analysis, computer games, entertainment, and medical applications. Also, research is conducted on educational games and on HCI for augmented and virtual reality (AR/VR) systems.